ELECTRON BEAM WELDING OF Ti_6Al_4V ALLOY

FORET Rudolf, HAVLÍK Petr

Brno University of Technology, Brno, Czech Republic, EU, foret@fme.vutbr.cz

Abstract

Titanium alloys and their weld joints find wide application, in particular in aircraft, automotive and chemical industries, because of their outstanding specific strength and corrosion resistance. The high reactivity of these alloys and the strong degradation effect of elements contained in the atmosphere (H, N and O) make it necessary for these alloys to be welded in protective atmospheres or in vacuum. From this viewpoint, Electron Beam Welding (EBW) is an advantageous welding technology, in large series production. In the paper, the effect is studied of the spot diameter and beam focusing on the penetration depth and the weld shape in the Ti6Al4V alloy. The results obtained are complemented with an analysis of the microstructure and mechanical properties (microhardness, tensile tests) measurements across the welds.

Keywords: Electron beam welding, Ti6Al4V alloy, shape and dimension of weld, microstructure, mechanical properties

1. INTRODUCTION

Titanium and its alloys are one of the best engineering materials for use in industrial applications [1, 2]. This is due to their properties such as excellent strength-to-density ratio, high fatigue strength, toughness, and good corrosion resistance. These properties make titanium alloys attractive for aerospace applications [3] and also for many chemical, marine, military and sport applications, in spite of the price of these alloys being relatively high.

The Ti6Al4V alloy is the most widely used α+β titanium alloy, accounting for more than 60 % of the world production of this alloy and serves as world standard in aerospace applications [4]. The mechanical and physical properties of this alloy are controlled by microstructural development during thermo-mechanical processing [5, 6]. At temperatures above 350 °C, particularly in molten state, titanium is very reactive with atmospheric oxygen, nitrogen, hydrogen, and carbon. These interstitial elements reduce ductility and toughness and increase strength and hardness [6]. Contamination by these elements during welding can be caused by poor preparation and cleaning of the joint and filler materials, poor shielding of the weld zone or by impurities in the gas.

Titanium may be joined by a variety of conventional fusion welding processes, but its chemical reactivity requires precaution in order to avoid contamination of the fusion and heat-affected zones. Fusion welding of titanium alloy is possible in inert gas shielded arc and high-energy beam welding processes such as EBW and plasma welding [7]. The EBW process is considered superior to others because of the deep and narrow weld zone, reduced heat-affected zone (HAZ) and high reliability. EBW is relatively often used for the welding of Ti alloys, since welding is carried out inside a chamber in which a vacuum is maintained to protect the weld from contamination. Great joint depth, which can be achieved with high beam power density ($1.5 \cdot 10^4$ - $1.5 \cdot 10^5$ $W \cdot mm^{-2}$), and the keyhole-mode welding increase the productivity and reduce heat input, when compared to the arc-welding processes [8].

The effect of accelerating voltage (U), beam current (I) and welding speed (v) on the depth of penetration and the whole geometry of the weld were studied in [9] for the Ti6Al4V alloy via a series of weld trials. The objective of the present study was to optimize the welding parameters of commercial Ti6Al4V alloy by EBW, namely the

influence of the spot diameter and the distance of EB focus from the surface, the size and shape of the weld (weld penetration, the width of the weld metal and HAZ), the microstructure and hardness of individual areas.

2. EXPERIMENTAL MATERIALS AND PROCEDURES

The Ti6Al4V alloy was produced by the VSMPO-AVISMA Corporation, Russia. Data on the chemical composition, given in **Table 1**, have been taken from a copy of the "Inspection Certificate".

Table 1 Chemical composition (in wt. %) of alloy Ti6Al4V

Al	V	Fe	O	C	N	H	Ti
6.46	4.11	0.21	0.166	0.007	0.004	0.0055	balance

Material for individual tests was cut from an 8x250x1000 mm sheet metal plate. EBW was carried out using the AG&COKGaA device with industry welding chamber K26 (a product of the German Probeam company). The parameters of the welds are given in **Table 2**, together with the designations of individual samples.

Table 2 Varying parameters of EBW

Specimen	Spot diameter (mm)	SURF (mA)	Specimen	Spot diameter (mm)	SURF (mA)
5	0.3	- 3	11	0.2	10
6	0.6	- 3	12	0.2	15
7	0.9	- 3	13	0.2	- 5
8	1.2	- 3	14	0.2	- 10
9	0.2	0	15	0.2	- 15
10	0.2	5	16	0.2	- 20

With all the samples, the welding speed was identical, 20 $mm \cdot s^{-1}$, and so were the beam current (18 mA), accelerating voltage (120 kV) and the working distance used. The term *spot diameter* used in **Table 2** corresponds to the diameter of electron beam circular scanning patterns, and the term *SURF* gives in the given case the values of mA corresponding roughly to the electron beam focusing above (+) and below (-) the surface of individual samples, in mm.

Specimens for the metallographic analysis were ground, polished and etched in Kroll's reagent (2 ml HF, 8 ml HNO_3, 92 ml distilled H_2O). The study of microstructures was carried out using a ZEISS AXIO light microscope and a ZEISS Ultra Plus scanning electron microscope equipped with EDS Oxford.

Tensile tests were carried out according to standard CSN EN ISO 6892-1 using ZWICK Z250 testing machine. Flat specimens DIN 50 125-E 8x14x60 were used. HV0.1 microhardness tests were conducted using the LECO.LM 274AT device.

3. RESULTS AND DISCUSSION

The microstructure of the Ti6Al4V in as-supplied state (annealed at 780°C/1h/air)) is formed by polygonal grains of the α-phase and, on a much smaller scale, by irregular configurations of the β-phase, which mainly occurs on the α-phase boundaries, as evident in **Figure 1**. Part of the α-phase is arranged in lines, with the β-phase occurring inside these grains. The α-phase is assumed to be the result of the transformation of the β-phase, which occurred at an annealing temperature of 780 °C. Via the EDS method it was established that the content of vanadium in the β-phase ranged between 18 and 22 wt. %, which testified to the high value of the coefficient of interphase distribution of vanadium between the two coexisting phases. For the sake of

completeness, it should be added that the aluminium content measured in the β-phase is within a narrow range of 2.5 - 4.8 wt. %. In the case of the chemical composition of the α-phase it is quite the contrary (8.6 - 9.6 wt.% Al and 2.8 - 3.3 wt. % V). The state described above is probably a non-equilibrium state.

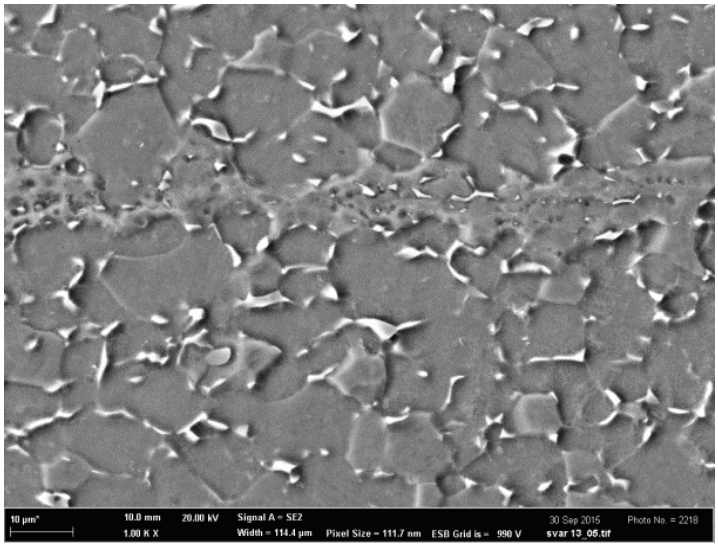

Figure 1 Microstructure of BM, etch. Kroll, SEM

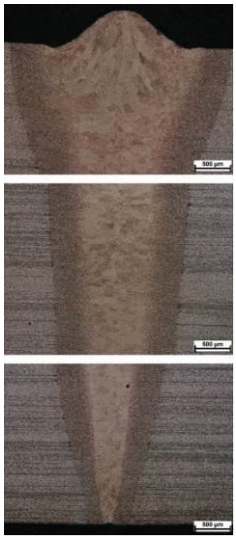

Figure 2 Weldment macrostructure

One of the pictures of the structure of the welds is given in **Figure 2**. Evaluating the structures of all the weld variants given in **Table 3** revealed that in the welds there were no discontinuities of the type of cracks and bubbles. The obtained set of pictures of weld structures made it possible to determine the weld depth, the shape and size of weld metal (WM) and heat affected zone (HAZ). The shapes and dimensions of the welds are given in **Figures 3** and **4** for individual sizes of the spot diameter, with the beam current, accelerating voltage and welding speed remaining constant. It is obvious from **Figures 3** and **4** that with increasing values of the spot diameter the weld depth decreases markedly while the width of weld metal (molten pool) increases. Changing analogously are also the shape and dimensions of the weld, i.e. the values of WM and HAZ, with the HAZ width almost not changing with the spot diameter value.

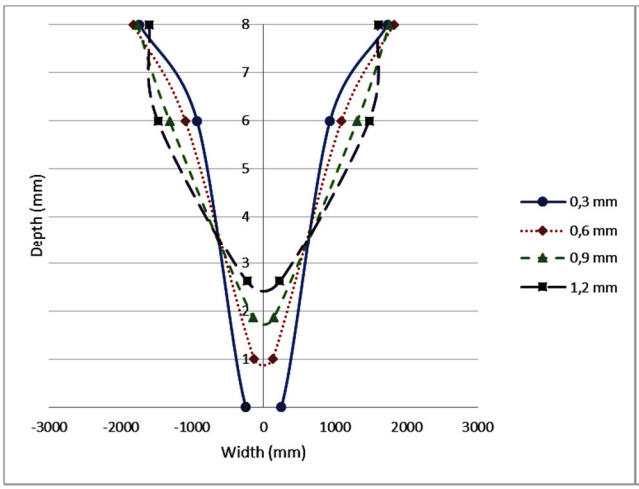

Figure 3 Influence of the "Spot" on the WM size and shape

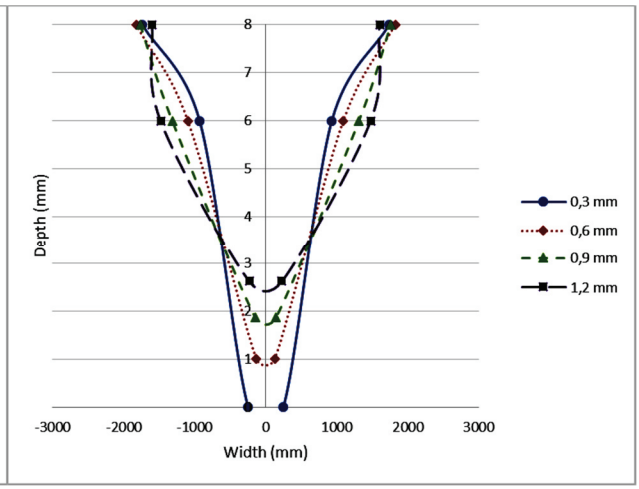

Figure 4 Influence of the "Spot" on the weld size and shape

A simple relation holds for the beam diameter, $d = s \cdot I/U$, where I is the beam current, U is the accelerating voltage, and s is a constant given by the electron gun optics. Thus in our case the beam diameter was constant.

If the beam diameter or the size of spot diameter increases, it can be expected that for a given beam energy given by the $U \cdot I$ product the energy will accumulate in a larger volume of material and, consequently, the weld depth will decrease. For a weld depth b the authors of [9] give the relation

$$b = C\frac{P}{TD}\sqrt{\frac{K}{vd}}, \tag{1}$$

where C - constant, P - beam power, T - melting point, D - thermal diffusivity, K - thermal conductivity, v welding speed. T, D and k are physical constants so that equation (1) can be rewritten in the form

$$b = CPC_1\sqrt{\frac{1}{vd}}, \tag{2}$$

where $C_1 = \sqrt{K}/TD$ is the material constant. In the given case, the beam diameter in equation (2) can be replaced by the spot diameter size; then with increasing spot diameter size the weld depth decreases and the weld shape is also changed, as can be seen from **Figures 3** and **4**. From the weld shape it can be concluded that for a spot diameter larger than 0.3 mm the mechanism of beam penetration operating in this case is predominantly by conduction-mode welding.

The growing value of positive focusing results in an increased diameter of the beam incident on a surface, which, in agreement with equation (2), led to the weld depth decreasing with increasing distance of focusing EB on the surface of metal sheet (quantified as the "SURF" value); by contrast, the width of WM and HAZ increased on the surface of metal sheet, with the overall shape of the weld remaining almost without change, **Figure 5**.

The growing size of negative focusing up to -10 mA led to increasing the weld depth; increasing the negative focusing still further had a reverse effect, the weld shapes then corresponded to the removal (predominantly by conduction) of the introduced heat, see **Figures 5** and **6**.

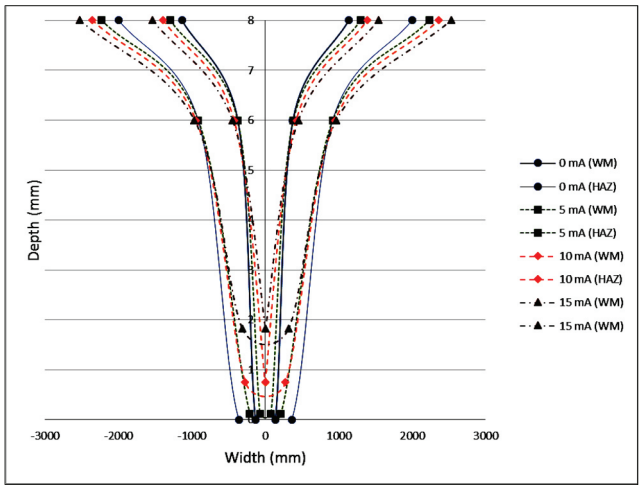

Figure 5 Shape and dimensions of the welds depending on the size of positive focusing

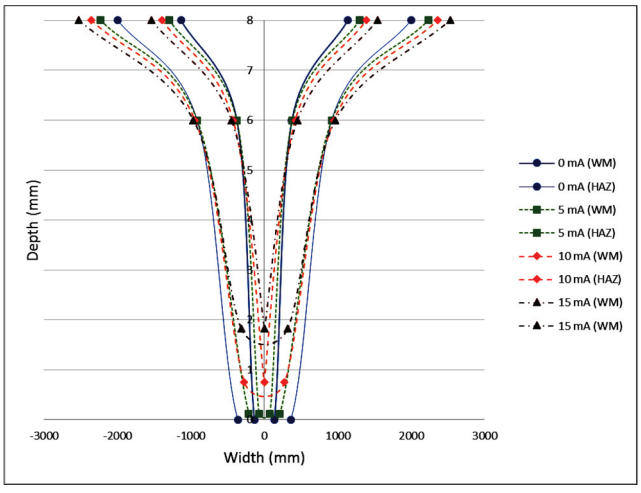

Figure 6 Shape and dimensions of the welds depending on the size of negative focusing

The microstructure of the weld metal is formed by α' martensite and, to a lesser degree, probably also by the β-phase, **Figure 7**. The microstructure of HAZ changes continuously from a predominantly martensitic structure with a major proportion of non-transformed β-phase (**Figure 8**) to a structure close to the basic

material, **Figure 9**. The latter is formed by a mixture of α-phase of acicular and also polygonal morphology with the β-phase, whose content is higher when compared with unaffected basic material.

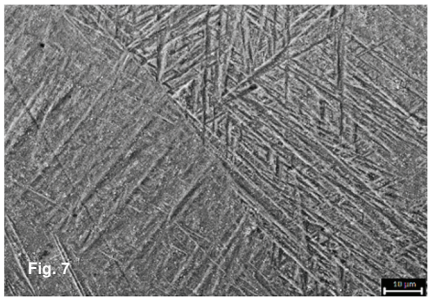

Figure 7 - Microstructure of WM

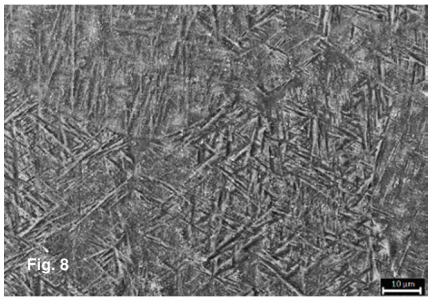

Figure 8 - Microstructure of HAZ (with HAZ followed by WM)

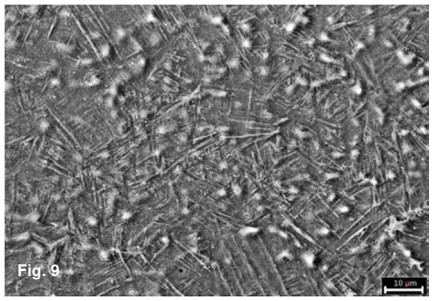

Figure 9 - Microstructure of HAZ (with HAZ followed by BM), etch. Kroll, SEM

The microstructure analysis was complemented with the measurement of the content of titanium, aluminium and vanadium across the weld interface, using the EDS method, on a line segment of 800 μm in length. From those analysis showed that in course of welding in a vacuum (pressure $3 \cdot 10^{-3}$ to $8 \cdot 10^{-3}$ Pa) there was no selective evaporation of any of the elements under analysis.

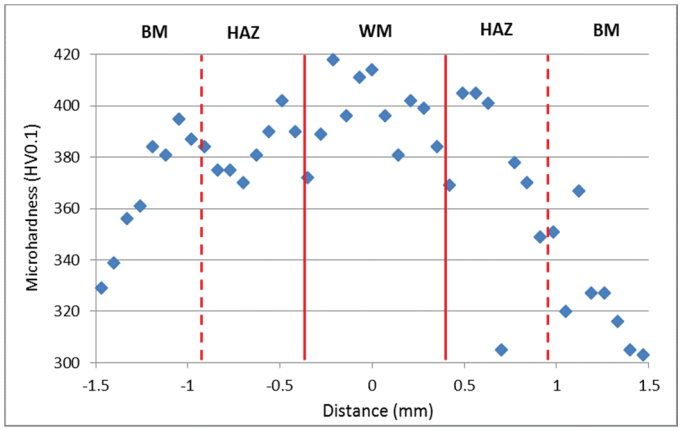

Figure 10 Microhardness HV0.1 across the weld, specimen no. 14

An example of the development of HV0.1 microhardness values across the weld of sample 14 can be seen in **Figure 10**. The values 380 - 420 HV0.1 correspond to the martensitic structure of WM in the whole set of samples; the same values were measured by the authors of [11]. In the welds examined, the differences in values between WM and BM amounted to as much as 70 HV0.1. The same differences were observed by the authors of [11], who additionally compared the results of tensile tests on samples taken from BM and EBW. In the case of EBW the fracture surfaces were in WM. It follows from the above comparison that the yield point values (960 MPa) and tensile strength values (1000 MPa) do not change but in WM there was a drop in the values of elongation (12.7→7.7 %), contraction (34.3→21.0) and impact energy (16→10 J).

Table 3 Results of tensile tests

Specimens	Yield strength $R_p0.2$ (MPa)	Tensile strength R_m (MPa)	Elongation A (%)
BM	930, 935, 924	988, 992, 984	13.2, 14.2, 14.7
weld 5	-	854, 855, 915	0.1, 0.1, 0.2
weld 13	919, 933, 925	922, 933, 925	0.3, 0.2, 0.2
weld 14	-, 913, 914	927, 913, 918	0.2, 0.2, 0.4

Significantly greater embrittlement was found on the assessed welds, as is evident from a comparison of the results of tensile tests on bars oriented transversely welded joints labelled 5, 13 and 14 (see **Table 3**) with the values shown in [11]. In both cases during tensile tests all joints failed in WM. "Plate shaped microstructure" was found in [11], while martensite prevailed in the WM of assessed welds. PWHT should contain annealing at a temperature up to 900 °C

4 CONCLUSION

The effect was studied of the spot diameter in the range of 0.3 - 1.2 mm as well as that of focusing in the interval -20 - +15 mA of the electron beam, under constant values of the beam current *I* (18 mA), accelerating voltage *U* (120 kV) and the welding speed *v* (20 mm/s) on the penetration depth and weld shape in the Ti6Al4V alloy. The study yielded the following knowledge:

1. Increasing size of the spot diameter has the same effect on the weld depth as the beam diameter, i.e. with increasing spot diameter size the depth of the weld decreases and the weld width increases, in the weld face area in particular.
2. Positive focusing of the electron beam has an analogous effect on the weld depth to that of the increasing spot diameter value. Increasing the negative focusing to -10 mA led to increased weld depth; increasing the negative focusing still further had the reverse effect.

The marked differences in the hardness values of WM (400HV0.1) and BM (335HV0.1) indicate a significant hardening of weld metal. This hardening and embrittlement concurrently was demonstrated by tensile tests. Mainly from performed tensile tests implies the necessity for post-weld heat treatment of real welds.

ACKNOWLEDGEMENTS

This work has been supported by project of BUT Brno, No. FSI-S-14-2427.

REFERENCES

[1] BOYER, R. R., WELSCH, G., COLLINGS, E. W. eds. *Materials Properties Handbook: Titanium and Titanium Alloys.* ASM International, Materials Park, OH, 1994, 1060 p.

[2] DONACHIE, M. J. *Titanium: A Technical Guide.* 2nd ed. ASM International, Materials Park, OH, 2000, 381 p.

[3] BOYER, R. R. An overview on the use of titanium in the aerospace industry. *Materials Science and Engineering*, 1996, A213, pp.103-114.

[4] BARREDA, J. L. et al., Electron beam welded high thickness Ti6Al4V plates using filler metal of different composition to the base plate. *Vacuum*, 2001, vol. 62, pp. 143-150.

[5] BANERJEE, S., MUKHOPADHYAY, P. *Phase Transformation, Examples from Titanium and Zirconium Alloys*, 1st ed. Elsevier Ltd., 2007, 813 p.

[6] LÜTJERING, G. Influence of processing on microstructure and mechanical properties of (α+β) titanium alloys. *Materials and Science Engineering,* 1998, vol. A243, pp.32-45.

[7] LIENERT, T. J., BABU, S. S., SIEWERT, T. A., ACOFF, V. L. eds. *ASM Handbook: Welding Fundamentals and Processes*, Vol. 6A. 1st ed., ASM International, Materials Park, OH: 2011, 920 p.

[8] SCHULTZ, H. *Electron Beam Welding.* 1st ed. Cambridge: Woodhead Publishing Ltd. 1993, 232 p.

[9] THOMAS, G. et al. Electron beam welding studies of 25-mm thick Ti-6Al-4V sections. *Welding Research Supplement,* August 1989, pp.336-341.

[10] BALASUBRAMANIAN, T. S. et al. Effect of welding processes on joint characteristics of Ti-6Al 4V alloy. *Science and Technology of Welding and Joining,* 2011, vol.16, no.8, pp. 702-708.